PHYSICAL REVIEW B **93**, 241307(R) (2016)

Spin noise of a polariton laser

I. I. Ryzhov,[1] M. M. Glazov,[2,1] A. V. Kavokin,[1,3,4] G. G. Kozlov,[1] M. Aßmann,[5] P. Tsotsis,[6] Z. Hatzopoulos,[6] P. G. Savvidis,[6,7] M. Bayer,[2,5] and V. S. Zapasskii[1]

[1]*Spin Optics Laboratory, St. Petersburg State University, 1 Ul'anovskaya, Peterhof, St. Petersburg 198504, Russia*
[2]*Ioffe Institute, 26 Polytechnicheskaya, St. Petersburg 194021, Russia*
[3]*Department of Physics and Astronomy, University of Southampton, Southampton SO17 1BJ, United Kingdom*
[4]*CNR-SPIN, Viale del Politecnico 1, I-00133 Rome, Italy*
[5]*Experimentelle Physik 2, Technische Universität Dortmund, D-44221 Dortmund, Germany*
[6]*Microelectronics Research Group, IESL-FORTH, P.O. Box 1385, 71110 Heraklion, Greece*
[7]*Department of Materials Science and Technology, University of Crete, P.O. Box 2208, 71003 Heraklion, Greece*

(Received 10 March 2016; revised manuscript received 16 May 2016; published 22 June 2016)

We report on experimental study of the exciton-polariton emission (PE) polarization noise below and above the polariton lasing threshold under continuous-wave nonresonant excitation. The experiments were performed with a high-Q graded $5\lambda/2$ GaAs/AlGaAs microcavity with four sets of three quantum wells in the strong-coupling regime. The PE polarization noise substantially exceeded in magnitude the shot-noise level and, in the studied frequency range (up to 650 MHz), had a flat spectrum. We have found that the polarization and intensity noise dependences on the pump power are strongly different. This difference is ascribed to the bosonic stimulation effect in spin-dependent scattering of the polaritons to the condensate. A theoretical model describing the observed peculiarity of the PE polarization noise is proposed.

DOI: 10.1103/PhysRevB.93.241307

Introduction. Nowadays, the term "laser" is applied to any device producing coherent, monochromatic, and unidirectional light [1]. It turns out that stimulated emission of radiation is not the only way to generate laser light. In *polariton lasers*, light is emitted spontaneously by a condensate of bosonic quasiparticles, exciton-polaritons, accumulated in a single quantum state [2–5]. Polariton lasers do not require an exciton-polariton population inversion, and the emission may result from the quasiequilibrium ensemble of exciton-polaritons. In a polariton laser, a semiconductor microcavity is excited nonresonantly, either optically or electrically. A gas of electrons and holes created in the cavity forms excitons, which subsequently thermalize, mainly through exciton-exciton interactions. Their kinetic energy is lowered by interactions with phonons, and they relax along the lower polariton dispersion branch. The polaritons finally scatter to their lowest-energy state where they accumulate because of the Bose stimulation. The coherence of the particles therefore builds up from an incoherent reservoir [2,5,6]. The polariton lasers emit light due to photon tunneling through the Bragg mirrors. This emission is spontaneous; however, the light going out has all the properties of a laser light: It is coherent, monochromatic, polarized, and unidirectional. The stimulated scattering of polaritons and polariton lasing have been realized in planar and micropillar GaAs, CdTe, and GaN microcavities [4,7–9]. Room-temperature operation has been demonstrated in GaN- [10] and ZnO-based [11,12] polariton lasers. Recently, polariton lasers with electrical injection of carriers have been realized [13,14]. This technological breakthrough opens ways to a new generation of optoelectronic devices based on the Bose-Einstein condensates of mixed light-matter quasiparticles. This fact attracts great interest to further research of fundamental properties of polariton emitters. Along with investigations of regular properties of such systems, such as small-signal modulation characteristics of an electrically pumped polariton laser [15], a great amount of important physical information is provided by studying their stochastic properties. The statistics of exciton-polaritons in polariton condensates has been widely studied through the second-order coherence measurements (see, e.g., Refs. [16,17]), here the spin noise in polariton condensates is studied experimentally. At the same time, specific parameters of spin noise are crucial for applications on one hand and provide fundamental understanding of the emitting state nature on the other. Theoretically, a giant polarization noise is expected in the polariton lasing regime [18]. The origin of the giant noise is in the stochastic formation and bosonic amplification of the polarization of exciton-polariton condensates [19,20]. Here we study the polariton emission (PE) noise in a quantum-well microcavity above the polariton lasing threshold under continuous-wave (cw) excitation. The main attention is paid to the polarization noise of the emission, carrying the most specific information about dynamics of the polariton formation, relaxation, as well as of their interactions. Polarization noise is characterized by strong magnitude and broad bandwidth. A strongly nonmonotonic dependence of the PE polarization noise power on the pump intensity is found and interpreted.

Experimental. In contrast to standard measurements in spin-noise spectroscopy (see, e.g., Refs. [21–24]), in this Rapid Communication we analyzed polarization fluctuations of secondary emission, rather than of a probe beam. The experiments were performed with a high-Q graded $5\lambda/2$ $GaAs/Al_{0.3}Ga_{0.7}As$ microcavity containing four sets of three 10-nm GaAs quantum wells, located at the antinodes of the cavity, and Bragg mirrors formed of $Al_{0.15}Ga_{0.85}As$/AlAs layers (see Ref. [25] for details). Strong exciton-photon coupling provided the opportunity to selectively detect emission from the lower polariton branch. Figure 1 shows the schematics of the experimental setup (a) and the reflectivity and emission spectra of the sample (b). Output emission of a cw Ti:sapphire laser (**1**) was focused on the sample (**2**) by a Helios-44M objective (**3**). The beam was incident on the sample at a

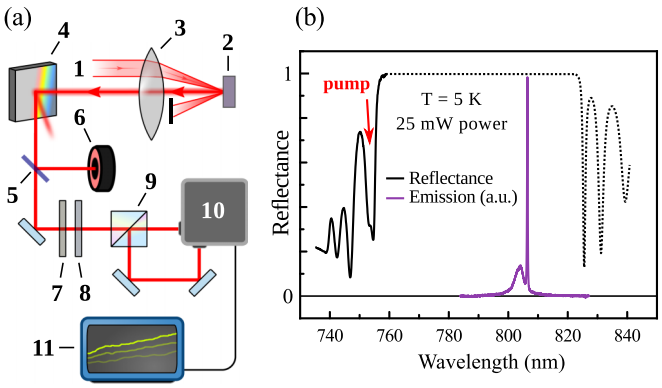

FIG. 1. (a) Schematics of the experimental setup (see the description in the text). (b) Reflection (black) and photoluminescence (purple) spectra of the microcavity structure. The solid curves represent the measured spectra, and the dashed line is a schematic of the sample's outer distributed Bragg reflector reflectivity.

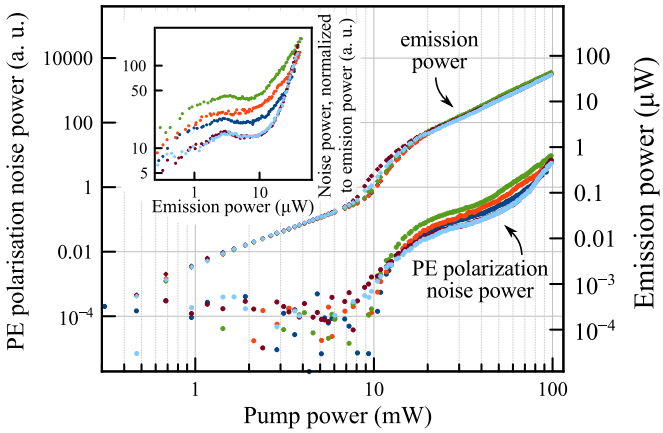

FIG. 2. Typical dependences of the PE power and polarization noise power on the pump intensity obtained for several randomly chosen points on the sample. The inset represents the dependence of polarization noise power normalized to the PE intensity on the PE intensity itself.

small angle to remove reflected light from the detector. The wavelength of the pump light was chosen to match the nearest to the stop-band reflectivity dip at about 755 nm. The diameter of the light spot on the sample was about 15 μm. The position of the spot on the sample was chosen to provide the most efficient polariton emission, which corresponded to small negative detunings.

The light emitted from the sample along its growth direction was sent to diffraction grating (**4**) to filter out the scattered pump light. A nonpolarizing beam splitter (**5**) diverts a fraction of the light beam to a power meter (**6**). The rest of the light beam is directed to the conventional spin-noise detection system (see, e.g., Ref. [24]) composed of the polarization beam splitter (**9**) and the balanced detector (**10**). The output signal of the latter is fed to the fast-Fourier-transform spectrum analyzer (**11**). We also used additional (half-wave and quarter-wave) phase plates (**7**) and (**8**) mounted in front of the beam splitter. The PE *intensity* noise was measured using a single detector of the balanced scheme without any preliminary polarization analysis. The bandwidth of the detectors used in this setup was either 100 or 650 MHz. The noise power spectrum was essentially flat up to $\gtrsim$650 MHz, hence, in our measurements we integrated the signal of the spectrum analyzer over a frequency range of 100 MHz to improve the measurements accuracy.

Results and discussion. The sample was found to be rather inhomogeneous: Changing position of the objective by a few microns could substantially change the characteristics of the PE. The emission spectrum typically contained several narrow peaks in the region of the lower polaritonic branch evolving independently with the pump power. Hence, in most cases, we detected the light from several emitters. This was implicitly revealed in power dependence of the noise magnitude (see below). Despite this inhomogeneity, the dependence of the PE intensity on the pump power was qualitatively the same for all spots on the sample, Fig. 2: In the region of low intensities, the PE power increased linearly, then, in the vicinity of 10 mW, it exhibited a sharp bend indicating the threshold of polariton lasing, after which it showed a monotonic superlinear growth with practically no essential features.

Polarization of the PE, in our experimental setup, was distorted by the diffraction grating, but since it did not show any noticeable birefringence, it could only slightly tilt the polarization plane or polarization ellipse. On the basis of polarization measurements with a quarter-wave plate installed in the pump beam, we have found that under linearly (or circularly) polarized pump, the PE was partially linearly (or, respectively, circularly) polarized.

The PE polarization noise proved to be fairly strong and covering a wide frequency range extending far beyond the bounds of the bandwidth of our detection system. At the same time it can be shown that, under our experimental conditions, for the width of the polarization noise spectrum 10–100 GHz, the ratio of power density of the polarization noise to that of the shot noise should be 1 to 2 orders of magnitude higher than what is observed experimentally. It agrees with the assumption that, generally, the detected light is contributed by many emitters, thus reducing the instantaneous degree of polarization.

Bearing in mind the description of polarized light using the Stokes vector $\boldsymbol{S} = (S_x, S_y, S_z)$, one can see that the light polarization fluctuations can be described just like the electron spin noise by the set of correlation functions of the Stokes vector components [18,26,27]. The light unpolarized on average may result from fluctuations of the polarization plane azimuth or from fluctuations of the light ellipticity. We performed additional measurements of ellipticity noise amplitude using the quarter-wave plate in the detection channel and found that the predominantly linearly or circularly polarized light (controlled by the pump polarization) mainly shows fluctuations of the polarization plane azimuth or ellipticity, respectively.

Typical dependences of the PE polarization noise power on the pump power are shown in Fig. 2. This plot reveals the threshold buildup in a more pronounced way than the PE power itself. After the threshold jump, all the curves show the same behavior with vague traces of peculiarities, which are revealed

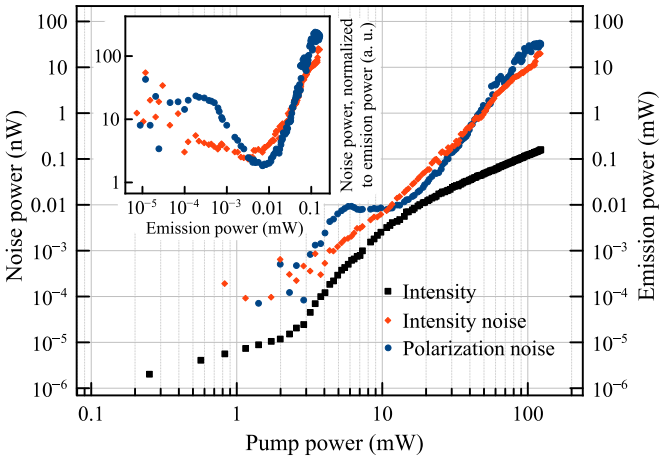

FIG. 3. An example of dependences of PE intensity (black squares), PE intensity noise (red rhombuses), and PE polarization noise (blue circles) on the pump power obtained at the same point on the sample. The inset shows intensity (red rhombuses) and polarization (blue circles) noise normalized to the emission intensity.

better once the polarization noise power is normalized to the PE intensity (see the inset in Fig. 2).

At some points on the sample, however, such peculiarities could be observed in a much more spectacular form as in Fig. 3 where the PE intensity (black squares), intensity noise (red rhombuses), and linear polarization noise (blue circles) are shown for the same point on the sample. We see that a strongly pronounced feature on the curve of the polarization noise is not revealed in two other dependences. This fact is additionally illustrated by the power dependences of the PE polarization and intensity noise (both normalized to the PE power) shown in the inset of Fig. 3. These normalized dependences allow one to reveal clearly these universal peculiarities of the PE polarization noise. Figure 4 shows several dependences of the intensity-normalized polarization noise power on the PE power for a few specially chosen points on the sample. We see that these dependences are systematically nonmonotonic, showing peaks at some level of excitation and subsequent decrease in the polarization noise with the PE power, followed by the growth at high emission/excitation powers. An interplay of individual emitters with different nonmonotonic contributions to the detected PE may smoothen the dependences.

The main features of the PE polarization noise and, especially, peculiarities of its power dependence can be qualitatively understood following the general model of polariton spin noise developed in Ref. [18]. First, due to the short polariton lifetime (∼1–10 ps), which was evaluated in Ref. [25], the intensity and polarization noise spectra are flat in the addressed frequency range, and it is sufficient to consider the noise contribution at zero frequency. For the polariton ensemble with $\langle N\rangle$ particles in the ground state (emission intensity $I \propto \langle N\rangle$) the intensity- and spin-noise powers, respectively, can be presented as [18]

$$(\delta I^2)_0 \propto \frac{\langle \delta N^2\rangle}{\Gamma_N}, \qquad (\delta P^2)_0 \propto \frac{\langle \delta N^2\rangle}{\Gamma_S}. \tag{1}$$

Here $\langle \delta N^2\rangle$ is the mean-square fluctuation of the particle number in the ground state, and Γ_N and Γ_S are the decay rates for fluctuations of the particle number and the Stokes vector components, respectively. Hereafter, we consider the fluctuations of the linear polarization which directly correspond to the fluctuations of the in-plane Stokes vector components S_x, S_y [18]. An increase in the pumping rate gives rise to an increase in the ground-state occupancy $\langle N\rangle$ and of the mean-square fluctuations. The latter is determined by the ground-state's statistics $g^{(2)}$,

$$\langle \delta N^2\rangle = \tfrac{1}{2}\langle N\rangle[1 + (g^{(2)} - 1)\langle N\rangle]. \tag{2}$$

For the coherent statistics relevant for polariton lasers operating above the threshold [29], $g^{(2)} = 1$ and $\langle \delta N^2\rangle \sim \langle N\rangle$. The decay of the particle number is governed by an interplay of the photon decay through the mirrors and the stimulated scattering towards the ground state. As a result, the fluctuations are supported by the stimulated scattering and $\Gamma_N = \Gamma_0/(1 + \langle N\rangle)$, where Γ_0 is the polariton decay rate in the linear regime [18]. As a result, for the intensity noise normalized to the ground-state occupancy (i.e., to the emission intensity) well above the thresholds $\langle N\rangle \gg 1$ and $g^{(2)} = 1$, one has

$$(\delta I^2)_0/\langle N\rangle \propto \langle N\rangle/\Gamma_0. \tag{3}$$

For the Stokes vector fluctuations decay rate one has [18] $\Gamma_S = \Gamma_N + \gamma_S$, where γ_S is the spin decoherence rate. For the in-plane Stokes vector components responsible for the linear polarization of emission an efficient channel of the decoherence is the self-induced Larmor precession [30,31] in the effective field caused by the fluctuating S_z component. For $\langle N\rangle \gg 1$ we obtain [18]

$$\gamma_S = |\alpha|\sqrt{\langle \delta N^2\rangle}, \tag{4}$$

where α is the effective constant of the polariton-polariton interaction for the parallel spin configuration; the interactions of polaritons with opposite spins are neglected, and the numerical coefficient is included in α. As a result, for the normalized polarization noise we get

$$(\delta P^2)_0/\langle N\rangle \propto \frac{\langle N\rangle}{\Gamma_0 + |\alpha|\langle N\rangle^{3/2}}. \tag{5}$$

The spin decoherence rate increases with increasing mean occupancy of the ground-state Eq. (4). It results in drastically different behaviors of the intensity and linear polarization noise: According to Eq. (3) the normalized intensity noise grows monotonously with $\langle N\rangle$, whereas the normalized noise of polarization $(\delta P^2)_0/\langle N\rangle$ behaves nonmonotonously with $\langle N\rangle$. First, it increases due to the decrease in Γ_S as a result of Bose stimulation and the corresponding decrease in the first term in the denominator of Eq. (5). Then, the interactions become sufficiently strong, the second term in the denominator of Eq. (5) starts to dominate, and the normalized polarization noise $(\delta P^2)_0/\langle N\rangle$ decreases. The further increase in the pump intensity may lead to the photon lasing when the strong coupling is lost. In this case, the interactions play a minor role and, consequently, the polarization and intensity fluctuations behave similarly. That is why the normalized polarization noise grows with the further increase in $\langle N\rangle$. It is illustrated in the inset of Fig. 4 where the results of the calculations are shown.

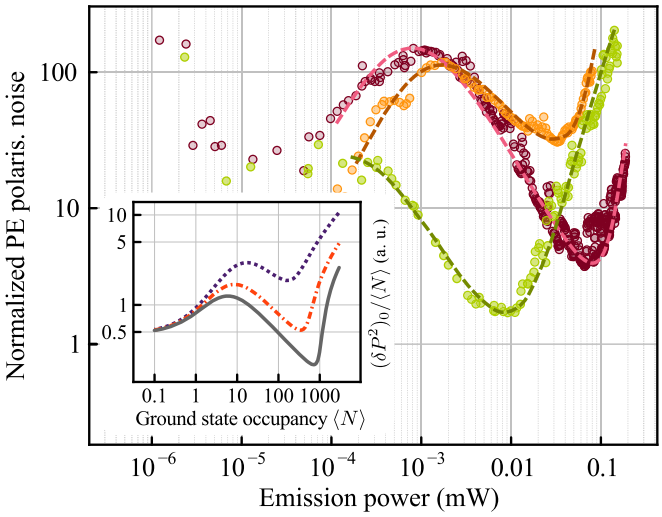

FIG. 4. Several (specially chosen) dependences of the normalized PE polarization noise power on the emission intensity. The dashed lines are guides to the eye. The inset represents normalized polarization noise as a function of the ground-state occupancy calculated for $g^{(2)} = 1$ and $\alpha/\Gamma_0 = 0.025$ (violet/dotted curve), 0.05 (red/dashed-dotted curve), and 0.075 (gray/solid curve). To model the transition for the photon lasing, we assumed that the interaction constant smoothly vanishes in the range of $\langle N \rangle$ from 100 to 200 (violet/dotted curve), 400 to 600 (red/dashed-dotted curve), and 900 to 1100 (gray/solid curve).

We stress that the presented model provides just a possible scenario, which qualitatively explains the experimental data. Due to the substantial inhomogeneity of the sample, the quantitative agreement is not possible in this simple model. Moreover, other factors, such as the dependence of the polariton second-order coherence $g^{(2)}$ on the pump power [29], anisotropic splitting of the polariton states, and the effect of interactions on the magnitude of the pseudospin-z component and, correspondingly, on the ellipticity fluctuations [18] should be taken into account in realistic modeling. Additionally, repulsive interparticle interactions may also suppress particle density fluctuations because such fluctuations are energetically unfavorable [32]. This might explain a slight reduction of the intensity noise (see the inset in Fig. 3). We do not address here the fluctuations below the threshold since the emission signals are very weak in this region.

The thresholdlike increase in spin fluctuations, well correlating with our results, has been reported in Refs. [33,34]. Unlike in our Rapid Communication, Refs. [33,34] used *pulsed* excitation and detected momentary polarizations corresponding to the peak intensities. Hence, the results of Ref. [33] correspond to the momentary fluctuations $\langle \delta S_\alpha^2 \rangle$ rather than to the zero-frequency spin-noise power Eq. (1). Moreover, the nonequilibrium fluctuations are not related to any susceptibility of the system [26,35], and there is no direct correlation between the cw values and the pulsed response. A further insight into the spin noise of polaritons requires measurements of spin-noise spectra in the whole range up to 10^2–10^3 GHz, e.g., by the ultrafast spin-noise spectroscopy [36].

Conclusion. In this Rapid Communication, we studied polarization noise of polariton emission of a quantum-well microcavity under cw excitation in the vicinity of the lasing threshold. In contrast to standard conditions of the spin-noise spectroscopy, we had to detect, in this case, strong polarization noise of a weakly polarized light, rather than small polarization fluctuations of a perfectly polarized beam. We have discovered that variations of the polarization noise with power and polarization of the pump reveal specific features hidden in the conventional intensity-related properties of the polariton emission. For instance, the polarization noise is apparently a much more sensitive quantity for mapping thresholds than the intensity or the intensity noise. We believe that these new opportunities of research provided by the polarization-noise technique will allow one in the future to obtain important information, inaccessible for other methods, about dynamics of the polariton Bose condensate under cw excitation.

Acknowledgments. Financial support from the SPbGU (Grant No. 11.38.277.2014), the RFBR, and DFG in the frame of International Collaborative Research Center TRR 160 (Project No. 15-52-12013) is acknowledged. The work was supported by RFBR Grant No. 16-52-150008. I.I.R. acknowledges RFBR Project No. 16-32-00593 and EU FP7-REGPOT-2012-2013-1 Grant No. 316165. M.M.G. also acknowledges partial support by the RFBR Project No. 14-02-00123, the Russian Federation President Grant No. MD-5726.2015.2, and the Dynasty Foundation. A.V.K. acknowledges the fellowship from EPSRC Established Career (Grant No. RP008833). The work was carried out using the equipment of SPbU Resource Center "Nanophotonics" (photon.spbu.ru).

[1] L. A. Coldren and S. W. Corzine, *Diode Lasers and Photonic Integrated Circuits* (Wiley, New York, 1995).

[2] *Exciton Polaritons in Microcavities*, edited by V. Timofeev and D. Sanvitto (Springer, New York, 2012).

[3] A. Imamoğlu, R. J. Ram, S. Pau, and Y. Yamamoto, Phys. Rev. A **53**, 4250 (1996).

[4] S. Christopoulos, G. Baldassarri Hoger von Hogersthal, A. J. D. Grundy, P. G. Lagoudakis, A. V. Kavokin, J. J. Baumberg, G. Christmann, R. Butte, E. Feltin, J.-F. Carlin, and N. Grandjean, Phys. Rev. Lett. **98**, 126405 (2007).

[5] A. V. Kavokin, J. J. Baumberg, G. Malpuech, and F. P. Laussy, *Microcavities* (Oxford University Press, Oxford, 2009).

[6] V. V. Belykh, N. N. Sibeldin, V. D. Kulakovskii, M. M. Glazov, M. A. Semina, C. Schneider, S. Höfling, M. Kamp, and A. Forchel, Phys. Rev. Lett. **110**, 137402 (2013).

[7] L. S. Dang, D. Heger, R. André, F. Bœuf, and R. Romestain, Phys. Rev. Lett. **81**, 3920 (1998).

[8] P. G. Savvidis, J. J. Baumberg, R. M. Stevenson, M. S. Skolnick, D. M. Whittaker, and J. S. Roberts, Phys. Rev. Lett. **84**, 1547 (2000).

[9] D. Bajoni, P. Senellart, E. Wertz, I. Sagnes, A. Miard, A. Lemaître, and J. Bloch, Phys. Rev. Lett. **100**, 047401 (2008).

[10] G. Christmann, R. Butte, E. Feltin, J.-F. Carlin, and N. Grandjean, Appl. Phys. Lett. **93**, 051102 (2008).

[11] F. Li, L. Orosz, O. Kamoun, S. Bouchoule, C. Brimont, P. Disseix, T. Guillet, X. Lafosse, M. Leroux, J. Leymarie, G. Malpuech, M. Mexis, M. Mihailovic, G. Patriarche, F. Reveret, D. Solnyshkov, and J. Zuniga-Perez, Appl. Phys. Lett. **102**, 191118 (2013).

[12] T.-C. Lu, Y.-Y. Lai, Y.-P. Lan, S.-W. Huang, J.-R. Chen, Y.-C. Wu, W.-F. Hsieh, and H. Deng, Opt. Express **20**, 5530 (2012).

[13] P. Bhattacharya, B. Xiao, A. Das, S. Bhowmick, and J. Heo, Phys. Rev. Lett. **110**, 206403 (2013).

[14] C. Schneider, A. Rahimi-Iman, N. Y. Kim, J. Fischer, I. G. Savenko, M. Amthor, M. Lermer, A. Wolf, L. Worschech, V. D. Kulakovskii, I. A. Shelykh, M. Kamp, S. Reitzenstein, A. Forchel, Y. Yamamoto, and S. Höfling, Nature (London) **497**, 348 (2013).

[15] M. Zunaid Baten, T. Frost, I. Iorsh, S. Deshpande, A. V. Kavokin, and P. Bhattacharya, Sci. Rep. **5**, 11915 (2015).

[16] J.-S. Tempel, F. Veit, M. Aßmann, L. E. Kreilkamp, A. Rahimi-Iman, A. Löffler, S. Höfling, S. Reitzenstein, L. Worschech, A. Forchel, and M. Bayer, Phys. Rev. B **85**, 075318 (2012).

[17] S. Kim, B. Zhang, Z. Wang, J. Fischer, S. Brodbeck, M. Kamp, C. Schneider, S. Höfling, and H. Deng, Phys. Rev. X **6**, 011026 (2016).

[18] M. M. Glazov, M. A. Semina, E. Y. Sherman, and A. V. Kavokin, Phys. Rev. B **88**, 041309 (2013).

[19] J. J. Baumberg, A. V. Kavokin, S. Christopoulos, A. J. Grundy, R. Butte, G. Christmann, D. D. Solnyshkov, G. Malpuech, G. Baldassarri Hoger von Hogersthal, E. Feltin, J.-F. Carlin, and N. Grandjean, Phys. Rev. Lett. **101**, 136409 (2008).

[20] D. Read, T. C. H. Liew, Y. G. Rubo, and A. V. Kavokin, Phys. Rev. B **80**, 195309 (2009).

[21] G. M. Muller, M. Oestreich, M. Romer, and J. Hubner, Physica E **43**, 569 (2010).

[22] J. Hubner, F. Berski, R. Dahbashi, and M. Oestreich, pss (b) **251**, 1824 (2014).

[23] S. A. Crooker, D. G. Rickel, A. V. Balatsky, and D. L. Smith, Nature (London) **431**, 49 (2004).

[24] V. S. Zapasskii, Adv. Opt. Photonics **5**, 131 (2013).

[25] P. Tsotsis, P. S. Eldridge, T. Gao, S. I. Tsintzos, Z. Hatzopoulos, and P. G. Savvidis, New J. Phys. **14**, 023060 (2012).

[26] M. M. Glazov, JETP **122**, 472 (2016).

[27] Here the light field can be considered as a classical wave, otherwise field operators should be properly ordered [28].

[28] H. Carmichael, *An Open Systems Approach to Quantum Optics*, Lecture Notes in Physics Monographs, Vol. 18 (Springer-Verlag, Berlin, Heidelberg, 1993).

[29] F. P. Laussy, G. Malpuech, A. Kavokin, and P. Bigenwald, Phys. Rev. Lett. **93**, 016402 (2004).

[30] D. N. Krizhanovskii, D. Sanvitto, I. A. Shelykh, M. M. Glazov, G. Malpuech, D. D. Solnyshkov, A. Kavokin, S. Ceccarelli, M. S. Skolnick, and J. S. Roberts, Phys. Rev. B **73**, 073303 (2006).

[31] I. A. Shelykh, A. V. Kavokin, Y. G. Rubo, T. C. H. Liew, and G. Malpuech, Semicond. Sci. Technol. **25**, 013001 (2010).

[32] Yu. Kagan and B. V. Svistunov, JETP **78**, 187 (1994).

[33] H. Ohadi, E. Kammann, T. C. H. Liew, K. G. Lagoudakis, A. V. Kavokin, and P. G. Lagoudakis, Phys. Rev. Lett. **109**, 016404 (2012).

[34] V. G. Sala, F. Marsault, M. Wouters, E. Galopin, I. Sagnes, A. Lemaître, J. Bloch, and A. Amo, Phys. Rev. B **93**, 115313 (2016).

[35] S. Gantsevich, V. Gurevich, and R. Katilius, Riv. Nuovo Cimento Soc. Ital. Fis. **2**, 1 (1979).

[36] J. Hubner, J. G. Lonnemann, P. Zell, H. Kuhn, F. Berski, and M. Oestreich, Opt. Express **21**, 5872 (2013).